Point Mutations at L1280 in Na$_v$1.4 Channel D3-S6 Modulate Binding Affinity and Stereoselectivity of Bupivacaine Enantiomers

CARLA NAU, SHO-YA WANG, and GING KUO WANG

Department of Anesthesiology, Friedrich-Alexander-University Erlangen-Nuremberg, Erlangen, Germany (C.N.); Department of Biological Sciences, State University of New York at Albany, Albany, New York (S.-Y.W.); and Department of Anesthesia Research Laboratories, Brigham and Women's Hospital, Harvard Medical School, Boston, Massachusetts (G.K.W.)

This article is available online at http://molpharm.aspetjournals.org

ABSTRACT

Local anesthetics (LAs) block voltage-gated sodium channels. Parts of the LA binding site are located in the pore-lining transmembrane segments 6 of domains 1, 3, and 4 (D1-S6, D3-S6, D4-S6). We suggested previously that residue N434 in D1-S6 interacts directly with bupivacaine enantiomers in inactivated channels because side-chain properties of different residues substituted at N434 correlated with changes in blocking potencies of bupivacaine enantiomers. Furthermore, mutation N434R exhibited significant stereoselectivity for block of inactivated channels that resulted from a selective decrease in block by S(−)-bupivacaine. In the present study, we analyzed the role of residue L1280 in D3-S6 of the rat skeletal muscle Na$_v$1.4 channel in interactions with the enantiomers of bupivacaine. We substituted native leucine at L1280 with amino acids of different physicochemical properties. Wild-type and mutant channels were expressed transiently in human embryonic kidney 293t cells and were investigated under whole-cell voltage clamp. Block of resting mutant channels by bupivacaine enantiomers revealed little difference compared with wild-type channels. Block of inactivated channels was increased in a mutation containing an aromatic group (L1280W) and decreased in mutations containing a positive charge (L1280K, L1280R). Surprisingly, mutants L1280E, L1280N, L1280Q, and L1280R exhibited significant stereoselectivity for block of inactivated channels. More surprisingly, stereoselectivity resulted from a selective decrease in block by R(+)-bupivacaine, in contrast to mutation N434R in D1-S6. We propose that in inactivated channels, residues L1280 in D3-S6 and N434 in D1-S6 interact directly with LAs and thereby face each other in the ion-conducting pore.

Voltage-gated Na$^+$ channels regulate the Na$^+$ conductance of excitable membranes that underlies the depolarizing phase of the action potential. The tertiary structure of the Na$^+$ channel α-subunit comprises four homologous domains (D1 to D4), each containing six α-helical transmembrane segments (S1 to S6) and an S5-S6 linker that forms a P-loop as a hairpin from the extracellular side. These P-loops line the outer part of the channel's pore and form the selectivity filter, whereas the S6 segments of each domain are believed to line the inner part of the channel's pore (Catterall, 2000). The highly positively charged S4 segments in each domain are postulated to serve as a voltage sensor (Stuhmer et al., 1989; Kontis et al., 1997). Their outward movements upon depolarization (Yang and Horn, 1995; Yang et al., 1996) are believed to induce conformational changes in the pore that result in channel activation. During the activation process, S6 segments are likely to exhibit rotational/lateral movements, as suggested for K$^+$ channels (Perozo et al., 1999; Jiang et al., 2002). Segments D3-S4 and D4-S4 were proposed to be important for coupling channel activation to fast inactivation (Cha et al., 1999; Sheets et al., 1999). The structural determinants of Na$^+$ channel fast inactivation are hydrophobic residues (Ile-Phe-Met) in the intracellular D3-D4 loop that serve as an inactivation gate (Vassilev et al., 1988; West et al., 1992; Eaholtz et al., 1994) and several residues at the intracellular end of D4-S6 (McPhee et al., 1994, 1995) and within intracellular S4-S5 loops of D3 (Smith and Goldin, 1997) and D4 (McPhee et al., 1998) that serve as an inactivation gate receptor.

LAs block the propagation of action potential by binding in the ion-conducting pore of voltage-gated Na$^+$ channels. LAs more avidly bind to open and inactivated channel states rather than to resting channel states, suggesting a binding site that converts from a low- to a high-affinity conformation during state transitions of the channel (Hille, 1977; Hondeghem and Katzung, 1977). Mapping of the LA binding

ABBREVIATIONS: LA, local anesthetic; HEK, human embryonic kidney.

site by means of alanine-scanning mutagenesis of the rat brain Na$_v$1.2 channel and electrophysiological experiments in the oocyte expression system revealed specific amino acid residues in segments D4-S6, D3-S6, and D1-S6 that are involved in binding of the LA etidocaine. The two hydrophobic aromatic residues phenylalanine (F1764) and tyrosine (Y1771) in D4-S6 (Ragsdale et al., 1994) and the amino acid residues L1465, N1466, and I1469 in D3-S6 (Yarov-Yarovoy et al., 2001) have been proposed to face the channel pore and to form the high-affinity binding site for this LA. Moreover, L1465, N1466, and I1469 in D3-S6 were suggested to be involved in voltage-dependent activation and coupling to closed-state inactivation. Recently, residue I409 in D1-S6 was proposed to also contribute minimally to the LA binding site (Yarov-Yarovoy et al., 2002), whereas none of the residues in D2-S6 was found to do so (Wang et al., 2001; Yarov-Yarovoy et al., 2002).

Lysine point mutations of the rat skeletal muscle Na$_v$1.4 channel expressed in human embryonic kidney (HEK) 293t cells confirmed the contribution of phenylalanine F1579 in D4-S6 (homologous to F1764 in Na$_v$1.2) to the binding of various LAs (Wright et al., 1998) and found S1276 and L1280 in D3-S6 (homologous to S1461 and L1465 in Na$_v$1.2) to be involved in binding of the enantiomers of the LA bupivacaine (Wang et al., 2000). In addition, N434 and L437 in D1-S6 were proposed to be critical for LA binding as well (Wang et al., 1998). A subsequent study creating mutations at N434 that vary the hydrophobicity, aromaticity, polarity, and charge at this site revealed an intriguing correlation between the physicochemical properties of the substituted residues and the changes in potency of bupivacaine enantiomers to block inactivated channels, suggesting a direct interaction of N434 with the positively charged moiety of LAs. Supporting this hypothesis was the finding that mutation N434R exhibited significant stereoselectivity for the block of inactivated channels that resulted from a selective decrease in block by $S(-)$-bupivacaine (Nau et al., 1999).

In the present work, we carried out a systematic analysis of the role of residue L1280 in D3-S6 of rat skeletal muscle Na$_v$1.4 channel in gating and block by the enantiomers of bupivacaine using a similar approach. Residue L1280 was chosen because both alanine and lysine mutations at this position had the most robust impact on binding of pore-blocking drugs to inactivated channels in previous studies (Wang et al., 2000; Yarov-Yarovoy et al., 2001). We substituted the native leucine by a series of amino acid residues that vary the physicochemical properties at this site. Wild-type and mutant channel α-subunits were expressed transiently in HEK293t cells and were investigated under whole-cell voltage clamp. As LA probes, we chose the enantiomers of bupivacaine because stereoisomers can been useful tools in receptor mapping. Figure 1 shows computer-generated three-dimensional molecular structures of $R(+)$- and $S(-)$-bupivacaine. The results of this study support the idea that in inactivated channels, residues L1280 in D3-S6 and N434 in D1-S6 both interact directly with LAs and thereby face each other in the ion-conducting pore.

Materials and Methods

Site-Directed Mutagenesis and Transfection. Mutagenesis of rat Na$_v$1.4 was performed with Na$_v$1.4-pcDNA1/amp by means of the

Transformer Site-Directed Mutagenesis Kit (BD Biosciences Clontech, Palo Alto, CA) as described previously (Nau et al., 1999). HEK 293t cells were transfected with Na$_v$1.4-pcDNA1 (5 μg) and reporter plasmid CD8-pih3m (1 μg) by the calcium phosphate precipitation method. After incubation for 12 to 15 h, cells were replated in 35-mm culture dishes. Transfected cells were used for experiments within 3 days. Transfection-positive cells were identified by immunobeads (CD-8 Dynabeads; Dynal Biotech, Oslo, Norway).

Chemicals and Solutions. $R(+)$- or $S(-)$-bupivacaine were gifts from Dr. Lars-Inge Olsson (AstraZeneca, Södertälje, Sweden). The drugs were dissolved in dimethyl sulfoxide to give stock solutions of 100 mM. The highest dimethyl sulfoxide concentration obtained was 1% and had no effect on Na$^+$ currents. Experiments were performed with an external solution containing 65 mM NaCl, 85 mM choline Cl, 2 mM CaCl$_2$, and 10 mM HEPES (adjusted to pH 7.4 with tetramethylammonium hydroxide) and a pipette solution containing 100 mM NaF, 30 mM NaCl, 10 mM EGTA, and 10 mM HEPES (adjusted to pH 7.2 with CsOH). The reversed Na$^+$ gradient was used to minimize the series resistance artifact, which is less serious with outward currents. After a gigaohm seal and a whole-cell voltage clamp were established, the cells were dialyzed for at least 15 min before data acquisition. Control and test solutions were applied with a multiple-barrel perfusion system.

Electrophysiological Technique and Data Acquisition. Na$^+$ currents expressed transiently in HEK293t cells were recorded at room temperature with the whole-cell configuration of the patch-clamp method. Patch pipettes were pulled from borosilicate glass tubes (TW150F-3; World Precision Instruments, Berlin, Germany) and heat-polished at the tip to give a resistance of 1.0 to 1.5 MΩ. Currents were recorded with an Axopatch 200B patch-clamp amplifier (Axon Instruments, Union City, CA), filtered at 5 kHz, and sampled at 20 kHz. Experiments were conducted under capacitance and series-resistance compensation. Leakage currents were subtracted by the P/−4 method. pCLAMP 8.0.1 software (Axon Instruments) was used for acquisition and analysis of currents. Microcal Origin 6.1 software (OriginLab Corp, Northampton, MA) was used to perform least-squares fitting and to create figures. Data are presented as mean ± S.E.M. or fitted value ± S.E. of the fit. An unpaired Student's t test (SigmaStat; SPSS Science, Chicago, IL) was used to evaluate the significance of changes in mean values. P values <0.05 were considered statistically significant.
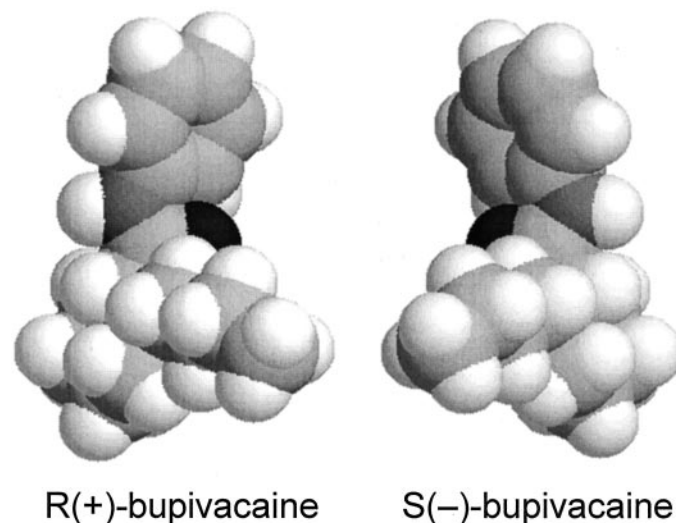

R(+)-bupivacaine   S(−)-bupivacaine

Fig. 1. Computer-generated three-dimensional molecular structures of $R(+)$- and $S(-)$-bupivacaine. The molecules were generated with the use of CORINA and RasMol software and are displayed in spacefill mode with Van der Waals radii.

Results

Effect of Point Mutations at L1280 on Channel Activation and Steady-State Inactivation. The following amino acid residues were chosen to substitute the native leucine at position L1280: alanine (A) with a small aliphatic residue; the sulfur- or hydroxyl-containing polar residues cysteine (C) and threonine (T); the polar residues asparagine (N) and glutamine (Q); the aromatic residues phenylalanine (F), tyrosine (Y), and tryptophan (W); the acidic, negatively charged residues aspartate (D) and glutamate (E); and the positively charged residues lysine (K) and arginine (R).

Wild-type and mutant channel α-subunits were expressed transiently in HEK293t cells and were investigated under whole-cell voltage clamp. Current density for wild-type was 253 ± 51 pA/pF. Mutants L1280A, L1280C, L1280D, L1280E, L1280K, L1280N, L1280Q, L1280R, L1280T, and L1280W expressed sufficient Na^+ currents for further analysis, whereas mutants L1280F and L1280Y expressed little or no Na^+ currents. Current densities for sufficiently expressing mutants all were significantly smaller compared with wild-type except for mutants L1280C and L1280N (Table 1). Current densities did not correlate with the volume or hydropathy index of substituted amino acids.

We first sought to assess whether point mutations in position L1280 alter gating properties of $Na_v1.4$ channels. Activation and inactivation properties of wild-type and mutant Na^+ channels were characterized with standard pulse protocols (Fig. 2A). In all mutant channels, the midpoint voltages of activation were significantly shifted rightward by approximately 6 to 22 mV compared with wild-type, except for mutant L1280D, in which the rightward shift was not statistically significant. The steepness of the activation curves were significantly decreased in all mutants compared with

wild-type channels except for mutants L1280C and L1280K, in which the decrease was not statistically significant (Table 1).

None of the mutants at L1280 tested showed any significant sustained current at the end of a 5-ms depolarization; they all inactivated completely from the open state. The midpoint voltages of steady-state inactivation were significantly shifted leftward in all mutants by approximately -7 to -12 mV compared with wild-type (Fig. 2B; Table 1).

Effect of Point Mutations at L1280 on State-Dependent Block by Bupivacaine Enantiomers. For all mutant channels, steady-state block by bupivacaine enantiomers was initially assessed with a three-step pulse protocol as described previously (Nau et al., 1999), allowing for direct estimation of block of resting and inactivated channels by LA drugs that unbind slowly from inactivated channels. In brief, Na^+ currents were evoked by 5-ms test pulses to $+50$ mV after 10-s conditioning prepulses between -180 and -50 mV (to allow binding to reach steady-state) and 100-ms intervals at the holding potential of -140 mV (to allow drug-free channels to recover from fast inactivation). Figure 3 shows normalized peak currents of wild-type and selected mutants in control and in the presence of 10 μM $R(+)$- or $S(-)$-bupivacaine as a function of the conditioning prepulse potential. As described previously for wild-type channels, slow inactivation was detectable in control after prepulses ≥ -100 mV. Block by 10 μM $R(+)$- or $S(-)$-bupivacaine reached plateaus after prepulses ≤ -120 and ≥ -70 mV, corresponding to the block of resting and inactivated channels, respectively. No stereoselectivity was detectable in the resting state, and little stereoselectivity was detectable in the inactivated state.

Mutant currents in control solution exhibited different de-

TABLE 1

Activation, inactivation kinetics, and current densities of $Na_v1.4$ wild-type (WT) and mutant channels

The fitted values ($\pm$ S.E. of the fit) for voltage dependence of activation ($E_{0.5}$, k_E) and fast inactivation ($h_{0.5}$, k_h) were determined as described in Fig. 2, A and B. For current densities (mean $\pm$ S.E.M.), peak currents at $+60$ mV were measured and divided by the membrane capacitance estimated by the acquisition software.

Channel	$E_{0.5}$	k_E	$h_{0.5}$	k_h	Current Density
			mV		*pA/pF*
WT	-34.7 ± 1.7	6.8 ± 0.7	-76.9 ± 2.0	5.7 ± 0.2	253 ± 51
	($n = 7$)	($n = 7$)	($n = 8$)	($n = 8$)	
L1280A	-16.4 ± 2.1	9.9 ± 0.5	-83.8 ± 1.2	6.0 ± 0.2	74 ± 10
	($n = 5$)	($n = 5$)	($n = 6$)	($n = 6$)	
L1280C	-24.9 ± 0.8	8.4 ± 0.4	-86.3 ± 1.7	5.8 ± 0.3	210 ± 73
	($n = 7$)	($n = 7$)	($n = 6$)	($n = 6$)	
L1280D	-27.9 ± 3.1	11.7 ± 0.6	-84.2 ± 1.3	7.5 ± 0.4	40 ± 10
	($n = 7$)	($n = 7$)	($n = 9$)	($n = 9$)	
L1280E	-19.5 ± 0.9	10.1 ± 0.6	-90.5 ± 1.8	6.8 ± 0.2	50 ± 11
	($n = 5$)	($n = 5$)	($n = 5$)	($n = 5$)	
L1280K	-20.4 ± 2.2	8.3 ± 0.5	-88.4 ± 2.1	6.5 ± 0.3	99 ± 17
	($n = 7$)	($n = 7$)	($n = 7$)	($n = 7$)	
L1280N	-6.5 ± 1.4	12.8 ± 0.8	-87.4 ± 2.0	6.6 ± 0.3	174 ± 35
	($n = 7$)	($n = 7$)	($n = 5$)	($n = 5$)	
L1280Q	-15.5 ± 2.6	11.6 ± 1.3	-83.6 ± 1.9	6.1 ± 0.2	60 ± 11
	($n = 8$)	($n = 8$)	($n = 6$)	($n = 6$)	
L1280R	-13.0 ± 3.9	14.5 ± 1.4	-93.1 ± 1.2	7.4 ± 0.3	50 ± 12
	($n = 7$)	($n = 7$)	($n = 6$)	($n = 6$)	
L1280T	-20.7 ± 1.3	10.0 ± 0.8	-88.4 ± 1.3	6.5 ± 0.3	127 ± 29
	($n = 8$)	($n = 8$)	($n = 7$)	($n = 7$)	
L1280W	-28.8 ± 1.2	9.1 ± 0.6	-86.1 ± 1.7	6.0 ± 0.4	109 ± 24
	($n = 8$)	($n = 8$)	($n = 8$)	($n = 8$)	
N343E	-43.7 ± 1.2	7.4 ± 0.4	-72.6 ± 0.9	4.9 ± 0.3	108 ± 26
	($n = 6$)	($n = 6$)	($n = 5$)	($n = 5$)	
N434Q	-36.6 ± 1.6	8.5 ± 0.3	-67.0 ± 1.8	6.3 ± 0.4	328 ± 67
	($n = 7$)	($n = 7$)	($n = 6$)	($n = 6$)	

grees of slow inactivation after prepulses ≥ -110 mV. This phenomenon is similar to that observed for mutations at N434, but it likewise did not correlate with the potency of bupivacaine to block inactivated channels.

Block of resting mutant channels by $R(+)$- or $S(-)$-bupivacaine revealed little differences compared with wild-type channels. Block of inactivated channels by $R(+)$- or $S(-)$-bupivacaine was slightly increased in mutant L1280W and was dramatically decreased in mutant L1280K. Surprisingly, mutants L1280E, L1280N, L1280Q, and L1280R exhibited significant stereoselectivity for block of inactivated channels. More surprisingly, stereoselectivity resulted from a selective decrease in the block of inactivated channels by $R(+)$-bupivacaine. This is in contrast to mutation N434R of D1-S6, in which stereoselectivity for block of inactivated channels resulted from a selective decrease in block by $S(-)$-bupivacaine.

To determine more accurately the potencies of bupivacaine enantiomers in blocking resting and inactivated channels, IC$_{50}$ values for block of wild-type and mutant channels by $R(+)$- and $S(-)$-bupivacaine were derived from concentration-inhibition experiments. A prepulse potential of -140 mV was deemed sufficient to estimate bupivacaine potency for resting channels. Potencies for inactivated channels were all estimated with a prepulse potential of -70 mV. At this

potential, block of L1280E, L1280N, L1280Q, and L1280R did not yet reach a plateau, so we might have slightly underestimated the block of inactivated channels in these mutants. The effects of 10 μM $R(+)$- and $S(-)$-bupivacaine on wild-type and selected mutant Na$^+$ currents elicited after prepulses to -140 and -70 mV are shown in Fig. 4A, and the IC$_{50}$ values derived from concentration-inhibition experiments are summarized in Fig. 4, B and C. The channels are arranged from top to bottom traces (Fig. 4A) and from left to right (Fig. 4, B and C) according to the hydropathy index of the substituted amino acid residue, beginning with the most hydrophobic. All IC$_{50}$ values are listed in Table 2, along with calculated ratios for stereoselective potencies.
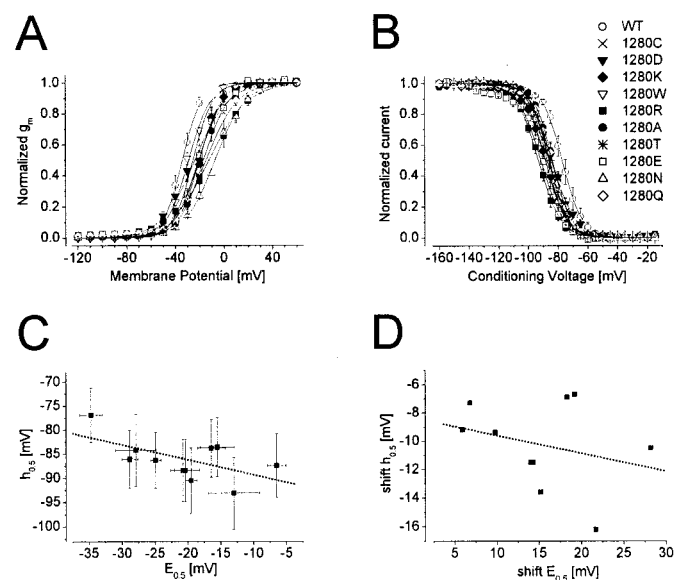

Fig. 2. Activation and steady-state inactivation of wild-type and mutant Na$_v$1.4 channels. A, Na$^+$ currents were evoked by 5-ms pulses ranging from -120 to $+50$ mV. Holding potential (V$_h$) was -140 mV. The interval between pulses was 20 s. The peak conductance (g$_m$) was estimated from the equation g$_m$ = I$_{Na}$/(E$_m$ − E$_{rev}$), where I$_{Na}$ is the peak current, E$_m$ is the corresponding voltage, and E$_{rev}$ is the estimated reversal potential. The data were least-squares fitted with the Boltzmann equation g$_m$/g$_{max}$ = 1/{1 + exp[(E$_{0.5}$ − E)/k$_E$]}, where g$_{max}$ is the maximum conductance, E$_{0.5}$ is the voltage at which g/g$_{max}$ = 0.5, and k$_E$ is the slope factor. The mean E$_{0.5}$ ± S.E.M. and k$_E$ ± S.E.M. values are given in Table 1. B, Na$^+$ currents were evoked by a 5-ms test pulse to $+50$ mV after 100-ms conditioning prepulses (E$_{pp}$) between -160 and -15 mV in 5-mV increments. Intervals between pulses were 20 s. V$_h$ = -140 mV. Peak currents evoked by a test pulse were measured, normalized, and plotted against the conditioning prepulse potential. The data were least-squares fitted by the Boltzmann equation y = 1/{1 + exp[(E$_{pp}$ − h$_{0.5}$)/k$_h$]}, where h$_{0.5}$ is the voltage at which y = 0.5 and k$_h$ is the slope factor. The mean h$_{0.5}$ ± S.E.M. and k$_h$ ± S.E.M. values are given in Table 1. Plots of E$_{0.5}$ values versus h$_{0.5}$ values (C) and values for shifts of E$_{0.5}$ versus shifts of h$_{0.5}$ (D) did not show any significant correlations (r = -0.59 and -0.28, respectively).
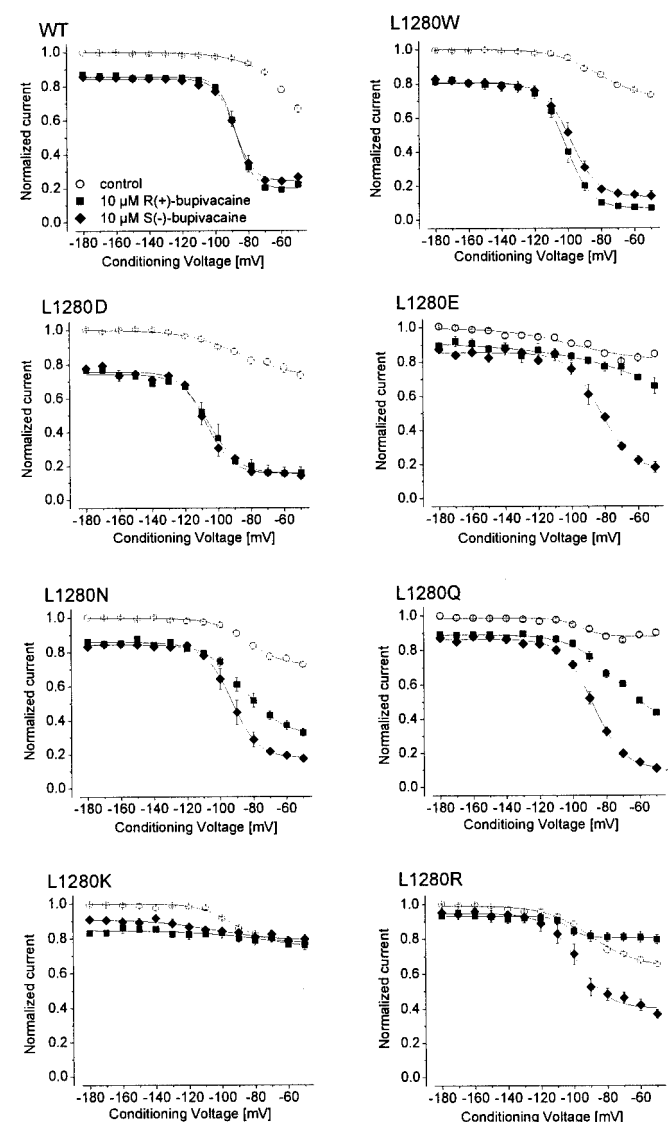
Fig. 3. State-dependent block of wild-type and mutant Na$_v$1.4 channels by 10 μM $R(+)$- or $S(-)$-bupivacaine. 10-s conditioning prepulses ranging from -180 to -50 mV were applied. Intervals (100-ms) at the holding potential of -140 mV were then inserted before delivery of the test pulses to $+50$ mV to evoke Na$^+$ currents. Pulses were delivered at 30-s intervals. Control currents (○) were normalized to the current obtained with a prepulse to -180 mV. The control data for experiments with $R(+)$-and $S(-)$-bupivacaine were combined. Currents obtained in the presence of 10 μM $R(+)$- (■) or $S(-)$-bupivacaine (◆) were normalized to the current obtained in control with the corresponding prepulse potential. Solid lines represent fits of the data to a Boltzmann function.

In resting channels, the blocking potency of $S(-)$-bupivacaine was slightly increased in L1280A, L1280T, and L1280D. Blocking potency of $R(+)$-bupivacaine was slightly decreased in L1280E, L1280K, and L1280R. In inactivated channels, the blocking potency of bupivacaine enantiomers was increased only in mutant L1280W. The blocking potency of $R(+)$-bupivacaine was selectively decreased in mutants L1280A, L1280N, L1280Q, L1280D, and L1280E. The blocking potency of both enantiomers was decreased in mutants L1280K and L1280R. Significant stereoselectivity was revealed in mutants L1280W, L1280A, L1280N, L1280Q, L1280D, L1280E, and L1280R and was greatest in mutants L1280R [$R(+)/S(-) = 7$], L1280E [$R(+)/S(-) = 5$], L1280Q [$R(+)/S(-) = 4$], and L1280N [$R(+)/S(-) = 2$]. Except for

Fig. 4. State-dependent block of wild-type and mutant $Na_v1.4$ channels by bupivacaine enantiomers. A, wild-type and mutant Na^+ currents in control solution (larger currents in each set of traces) and in the presence of 10 μM $R(+)$- and $S(-)$-bupivacaine (smaller currents in each set of traces). The same pulse protocol as described in the legend to Fig. 3 was used with conditioning prepulses to −140 mV for block of resting channels (E_{pp} = −140 mV, left column) and −70 mV for block of inactivated channels (E_{pp} = −70 mV, right column). B and C, affinities of resting (B) and inactivated (C) wild-type and mutant channels toward bupivacaine enantiomers. The IC_{50} values (fitted values ± S.E.M.) were obtained from concentration-inhibition experiments. Here, the same pulse protocol as that described in Fig. 3 was used with conditioning prepulses to −140 mV for block of resting channels and −70 mV for block of inactivated channels. The peak Na^+ currents were measured in different drug concentrations, normalized with respect to peak currents in control, and plotted against the drug concentration. The data were least-squares fitted with the Hill equation. The mean ± S.E.M. of Hill coefficients was 0.98 ± 0.02, with a minimum of 0.76 and a maximum of 1.40. For the final fit, the Hill coefficient was constrained to 1.0. Half-maximum inhibiting concentrations (IC_{50}) ± S.E.M. are given in Table 2. The channels are plotted from left to right according to their hydropathy index (Hopp and Woods, 1981; W, −3.4; L, −1.8; C, −1.0; A, −0.5; T, −0.4; N, 0.2; Q, 0.2; D, 3.0; E, 3.0; K, 3.0; and R, 3.0). *, statistically significant difference in IC_{50} values between $R(+)$- and $S(-)$-bupivacaine ($P < 0.5$); ■, statistically significant change in IC_{50} values for the enantiomer compared with the corresponding IC_{50} value in wild-type channels ($P < 0.5$).

mutation L1280W, stereoselectivity resulted from a selective decrease in block of inactivated channels by $R(+)$-bupivacaine. As mentioned previously, this is in contrast to the findings in mutation N434R of D1-S6, in which stereoselectivity for block of inactivated channels resulted from a selective decrease in block by $S(-)$-bupivacaine (Nau et al., 1999). In mutant N434R, the charge, size, and orientation of atoms and bonds in the guanidinium group of arginine were held responsible for bupivacaine stereoselectivity. Effects of substituting native asparagine in position N434 by glutamate and glutamine were not investigated in that study.

Effects of Mutations N434E and N434Q on Activation, Steady-State Inactivation, and State-Dependent Block by Bupivacaine Enantiomers. To test whether glutamate and glutamine are likewise able to cause bupivacaine stereoselectivity while residing in position N434, we created mutations N434E and N434Q and studied their gating properties and state-dependent interaction with bupivacaine enantiomers.

Activation and inactivation properties of mutations N434E and N434Q were characterized with standard pulse protocols as described in Fig. 2. Original current traces of N434E and N434Q recorded to estimate activation properties are shown in Fig. 5, A and B, respectively, and the corresponding activation curves are shown in Fig. 5C. Mutation N434E exhibited rectification at positive voltages and significant sustained currents at the end of a 5-ms depolarization (Fig. 5A). The midpoint voltage of activation was shifted leftward by −6 mV compared with wild-type channels. Activation properties of N434Q were unchanged compared with wild-type channels. The midpoint voltage of steady-state inactivation was unchanged in mutant N434E and was shifted rightward by 10 mV in mutant N434Q compared with wild-type channels (Fig. 5D; Table 1).

The effects of 10 μM $R(+)$- and $S(-)$-bupivacaine on mutants N434E and N434Q elicited after prepulses to −140 and −70 mV are shown in Fig. 6, A and B. The normalized peak currents of mutant N434E and N434Q in control and in the presence of 10 μM $R(+)$-bupivacaine and $S(-)$-bupivacaine as a function of different conditioning prepulse potentials are shown in Fig. 6, C and D. Significant slow inactivation was detectable in control channels after prepulses ≥−90 and ≥−80 mV, respectively, that was more pronounced than in L1280 mutant channels. Block of resting channels by $R(+)$- or $S(-)$-bupivacaine was decreased in mutant N434E and was unchanged in mutant N434Q. In mutant N434E, block of inactivated channels by $S(-)$-bupivacaine was selectively decreased, resulting in a significant stereoselectivity. In mutant N434Q, block of inactivated channels was decreased for both bupivacaine enantiomers compared with wild-type channels. In both mutants, block after prepulses of −50 mV was less than after prepulses of −70 mV. This decrease in block could be caused by a lower affinity of slow inactivated channels than fast inactivated channels for bupivacaine. Alternatively, a modest amount of channel activation induced by prepulses >−70 mV could result in knockout of some drug molecules by external Na^+ ions. The IC_{50} values obtained from concentration-inhibition experiments in these mutations are listed, along with mutations in L1280, in Table 2.
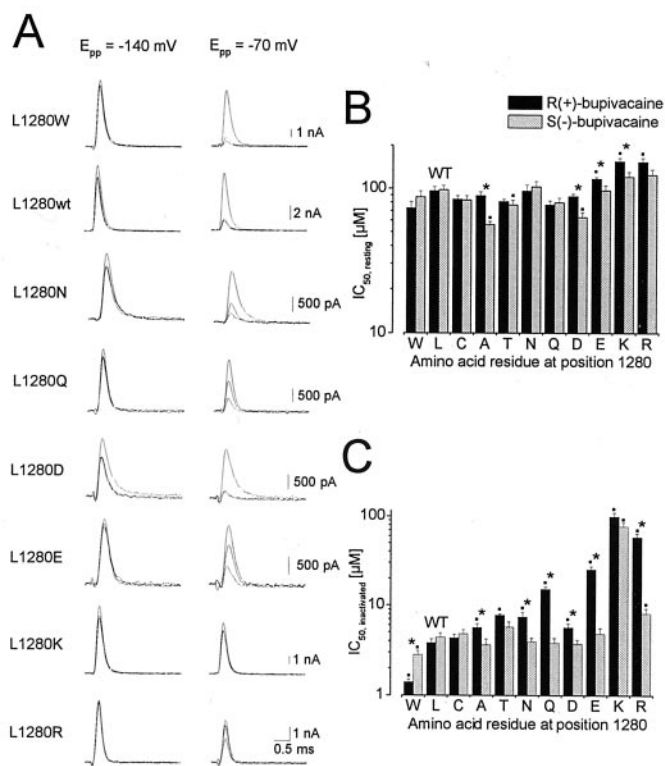
Discussion

Our data demonstrate that, similar to point mutations at N434 in D1-S6, point mutations at L1280 in D3-S6 had significant effects on both voltage-dependent activation and steady-state inactivation and on potencies of bupivacaine enantiomers to block resting and inactivated Na$_v$1.4 channels.

Role of Residue L1280 in Voltage-Dependent Activation and Steady-State Inactivation. Alanine mutations in the inner two thirds of D3-S6 were shown previously to cause periodic positive and negative shifts in the voltage dependence of activation (Yarov-Yarovoy et al., 2001). Mutation L1465A in Na$_v$1.2 channels (homologous to L1280 in Na$_v$1.4 channels), causing a positive shift, was reasoned to belong to a group of mostly hydrophobic residues on one side of the α-helical segment D3-S6 that faces the lumen of the pore in the activated and inactivated state and interacts with surrounding transmembrane segments in D3 in the resting state (Yarov-Yarovoy et al., 2001).

We show here that all mutations at L1280 cause positive shifts in the voltage-dependent activation and negative shifts in steady-state inactivation. However, our data do not reveal a clear relationship between shifts in activation or steady-state inactivation and the physicochemical properties of the substituted residues. These findings may indicate that the native aliphatic nonpolar residue leucine at position L1280 is involved in a highly specific intramolecular interaction that is required for normal activation and inactivation gating. Furthermore, our data do not reveal a significant correlation between positive shifts of activation and negative shifts of steady-state inactivation (Fig. 2, C and D). Thus, residue L1280 is differentially involved in the process of activation and inactivation. The incomplete inactivation from the open

state observed in mutation N434E is consistent with the proposed importance of residues at the intracellular end of segment D1-S6, among others, for closure of the fast inactivation gate (Yarov-Yarovoy et al., 2002). The peculiar rectification at positive voltages in mutation N434E (Fig. 5, A and C) might be caused by an interference of the glutamate residue with intracellular Na$^+$ ions and supports the idea that residue N434 is located close to the intracellular entry of the pore.

Role of Residue L1280 in State-Dependent Block by Bupivacaine Enantiomers. In this study, block of resting and inactivated channels by bupivacaine enantiomers could be clearly separated and directly measured in both wild-type and mutant channels. As demonstrated previously, LA affinities of resting and inactivated channels measured at strongly negative (≤ -140 mV) and less negative potentials (≥ -70 mV), respectively, are not affected by shifts in the voltage dependence of steady-state inactivation (Wright et al., 1999). Block of inactivated channels was measured after 10-s conditioning prepulses to -70 mV, which induced some degree of slow inactivation in wild-type and mutant channels. Thus, slow inactivated channels may have contributed to the block designated as block of inactivated channels. However, similar to mutations at N434 in D1-S6, shifts in fast and slow inactivation in mutations at L1280 in D3-S6 did not correlate with changes in block by bupivacaine enantiomers.

As shown previously for mutations at N434 in D1-S6 (Nau et al., 1999) and other mutations of residues presumably involved in LA binding in D3-S6 (Yarov-Yarovoy et al., 2001) and D4-S6 (Ragsdale et al., 1994), mutations at L1280 in D3-S6 affected block of resting and inactivated channels by bupivacaine enantiomers differently. Most resting mutant

TABLE 2

IC$_{50}$ values for bupivacaine block of resting and inactivated Na$_v$1.4 wild-type (WT) and mutant channels

The IC$_{50}$ values (fitted value $\pm$ S.E. of the fit) for the resting and inactivated states were obtained as described in Fig. 4, B and C.

Channel;	IC$_{50}$ Resting			IC$_{50}$ Inactivated		
	R(+)	S(−)	R(+)/S(−)	R(+)	S(−)	R(+)/S(−)
	μM			*μM*		
WT	96 ± 7 (n=8)	98 ± 7 (n = 8)	1.0	3.8 ± 0.4 (n = 8)	4.4 ± 0.5 (n = 8)	0.9
L1280A	89 ± 6 (n=5)	56 ± 3 (n = 7)	1.6	5.6 ± 0.6 (n = 5)	3.6± 0.6 (n = 6)	1.6
L1280C	84 ± 5 (n=5)	83 ± 6 (n = 5)	1.0	4.3 ± 0.4 (n = 5)	4.8 ± 0.5 (n = 5)	0.9
L1280D	88 ± 4 (n=4)	63 ± 5 (n = 5)	1.4	5.6 ± 0.6 (n = 4)	3.7 ± 0.4 (n = 5)	1.5
L1280E	117 ± 3 (n=5)	97 ± 8 (n = 5)	1.2	25 ± 2 (n = 5)	4.8 ± 0.7 (n = 5)	5.2
L1280K	155 ± 9 (n=5)	121 ± 10 (n = 5)	1.3	99 ± 10 (n = 5)	77 ± 8 (n = 5)	1.3
L1280N	96 ± 10 (n=5)	103 ± 9 (n = 5)	0.9	7.4 ± 0.9 (n = 5)	3.9 ± 0.4 (n = 5)	1.9
L1280Q	77 ± 5 (n=5)	80 ± 6 (n = 5)	1.0	15 ± 1 (n = 5)	3.8 ± 0.5 (n = 5)	3.9
L1280R	153 ± 11 (n=5)	125 ± 11 (n = 5)	1.2	58 ± 6 (n = 5)	8.1 ± 1.1 (n = 5)	7.2
L1280T	81 ± 3 (n=6)	77 ± 6 (n = 7)	1.1	7.7 ± 0.3 (n = 5)	5.7 ± 0.8 (n = 6)	1.4
L1280W	73 ± 8 (n=5)	87 ± 9 (n = 5)	0.8	1.4 ± 0.1 (n = 5)	2.8 ± 0.3 (n = 5)	0.5
N434E	189 ± 8 (n=5)	263 ± 10 (n = 5)	0.7	3.1 ± 0.3 (n = 5)	7.5 ± 1.1 (n = 5)	0.4
N434Q	94 ± 8 (n=5)	120 ± 8 (n = 5)	0.8	12 ± 2 (n = 5)	12 ± 2 (n = 5)	1.0

channels showed a higher affinity for bupivacaine than did resting wild-type channels. For alanine mutations in D3-S6, it was suggested that in resting channels, additional space is created for the drug molecule to reach its binding site (Yarov-Yarovoy et al., 2001). Our findings give additional support to the idea that the orientation of the side chain of the residues is likely to change in response to gating movements of S6 segments so that LAs might interact differently with relevant residues depending on channel state, as suggested for residues in D4-S6 (Li et al., 1999).

Mutations in N434 revealed an intriguing correlation between the physicochemical properties of the substituted residues and the changes in potency of bupivacaine enantiomers to block inactivated channels, consistent with a direct inter-

Fig. 5. Activation and steady-state inactivation of mutants $Na_v1.4$-N434E and $Na_v1.4$-N434Q. Na^+ currents through mutants $Na_v1.4$-N434E (A) and $Na_v1.4$-N434Q (B) were evoked by 5-ms pulses ranging from -120 to $+50$ mV from a holding potential of $V_h = -140$ mV. C and D, data for activation and steady-state inactivation of mutants $Na_v1.4$-N434E and $Na_v1.4$-N434Q were obtained as described in Fig. 2, A and B, respectively.
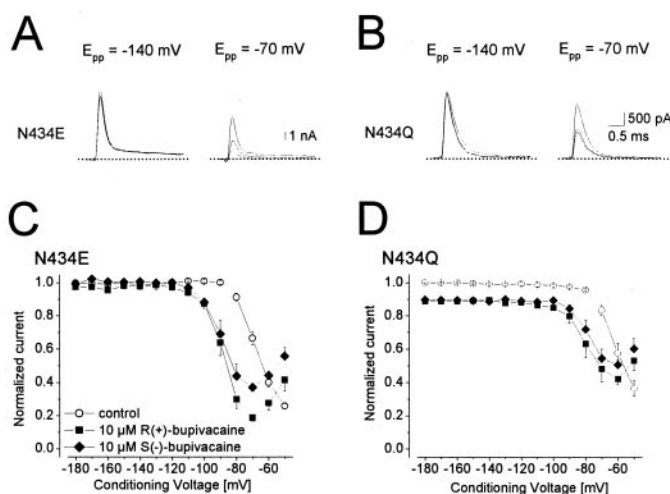
Fig. 6. State-dependent block of $Na_v1.4$-N434E and $Na_v1.4$-N434Q by bupivacaine enantiomers. A and B, Na^+ currents in control (larger currents in each set of traces) and in the presence of 10 μM $R(+)$- and $S(-)$-bupivacaine (smaller currents in each set of traces) were obtained as described in Fig. 4A. C and D, data of normalized $Na_v1.4$-N434E and $Na_v1.4$-N434Q currents in control channels ($\bigcirc$) and with 10 μM $R(+)$- ($\blacksquare$) and $S(-)$-bupivacaine ($\blacklozenge$), plotted as a function of the conditioning prepulse potential, were obtained as described in Fig. 3.

action of N434 with the positively charged amino group of bupivacaine (Nau et al., 1999). Bupivacaine block of inactivated channels was enhanced for mutations carrying an aromatic residue and a negatively charged residue, presumably through cation-π electron and electrostatic interaction with the positively charged moiety of bupivacaine, respectively. Bupivacaine block of inactivated channels was decreased for mutations carrying a positively charged residue, presumably through electrostatic charge-charge repulsion.

The data for mutations at L1280 show striking similarities to those for mutations at N434. Bupivacaine block of inactivated channels was likewise enhanced in mutation L1280W carrying an aromatic residue. Unfortunately, two other mutations of that type, L1280F and L1280Y, did not express sufficient current for further analysis. Bupivacaine block of inactivated channels was likewise decreased in mutations L1280K and L1280R carrying a positively charged residue. These finding suggest an interaction of residue L1280 in D3-S6 with LAs similar to that of residue N434 in D1-S6.

However, in contrast to mutation N434D, bupivacaine block of inactivated channels was not increased in mutation L1280D but was unchanged for $S(-)$-bupivacaine and slightly decreased for $R(+)$-bupivacaine. Mutation L1280E, carrying another negatively charged but larger residue, revealed a similar pattern. Here, block by $R(+)$-bupivacaine was substantially decreased, resulting in a significant bupivacaine stereoselectivity. A comparable result was obtained for mutation N434E, in which block by $S(-)$-bupivacaine was selectively decreased, resulting in a moderate bupivacaine stereoselectivity. These data indicate that, besides electrostatic interactions at both positions L12380 in D3-S6 and N434 in D1-S6, the size and the chemical structure of the residue might also play an important role in binding interactions. Altogether, data from mutations at either N434 or L1280 provide compelling evidence that, in the inactivated state, residues N434 and L1280 directly interact with LAs.

It is interesting that mutation L1465A in the rat brain $Na_v1.2$ channel, which corresponds to L1280A in the rat skeletal muscle $Na_v1.4$ channel, showed significantly reduced affinity of inactivated channels for the LA etidocaine in electrophysiological experiments in the oocyte expression system (Yarov-Yarovoy et al., 2001). In our experiments, block of resting and inactivated channels by bupivacaine enantiomers in mutation L1280A was only slightly changed compared with wild-type channels. Several explanations may account for these differences. First, homologous residues in different Na^+ channel isoforms, specifically in $Na_v1.2$ and $Na_v1.4$, may play disparate roles in LA binding. Second, the type of expression system might affect the actions of LAs on Na^+ channels. For example, differences between expression systems may reflect different post-translational modifications of channels. Third, leucine at position L1280/L1465 may interact differently with drug-specific moieties in LA molecules such as etidocaine and bupivacaine.

There are two striking differences in stereoselectivity induced by mutations at positions L1280 and N434. First, stereoselectivity was more pronounced in mutations at L1280. Second, stereoselectivity in L1280 was caused by a selective decrease in block by $R(+)$-bupivacaine, whereas in N434, it was caused by a selective decrease in block by $S(-)$-bupivacaine.
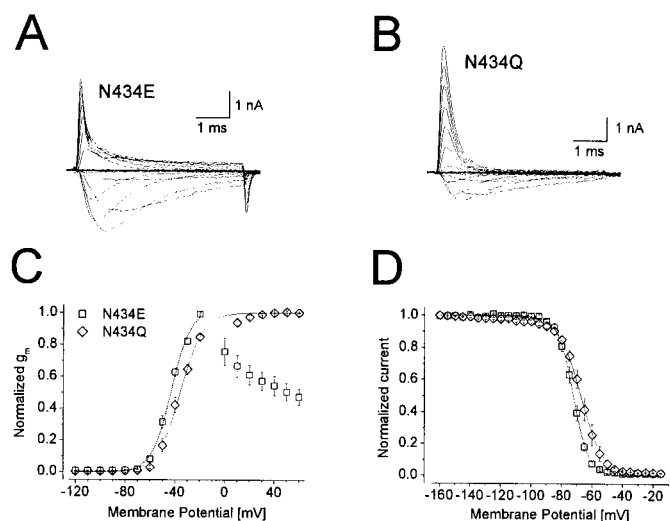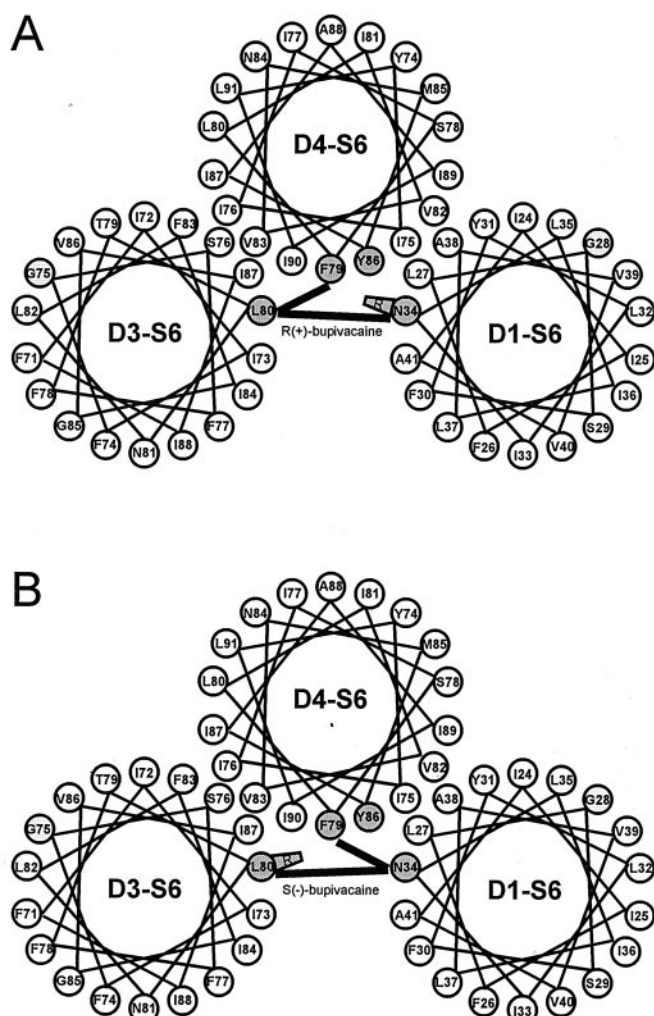
The amount of stereoselectivity $[R(+)/S(-)]$ for L1280R,

Fig. 7. Top view of the Na$^+$ channel in the inactivated state showing the axial position of residues in the α-helical segments D1-S6, D3-S6, and D4-S6, and the orientation of $R(+)$- (A) or $S(-)$-bupivacaine (B) within the channel's pore. The rectangular box with the "R" symbolizes the steric hindrance introduced by substituting N434 in D1-S6 (A) or L1280 in D3-S6 (B) with the amino acid residue arginine.

responsible for the flexibility of other S6 segments in the channel opening (Jiang et al., 2002).

We propose that the guanidinium group of arginine, the carboxylic acid moiety of glutamate, or the acid amide moiety of glutamine introduce a steric hindrance at both positions N434 in D1-S6 and L1280 in D3-S6 so that the inhibitory effect of either $R(+)$- or $S(-)$-bupivacaine is disrupted, depending on which segment is carrying the mutation. In other words, only one of the enantiomers is able to align appropriately at the binding site in the presence of a steric hindrance at position L1280 or N434 (Fig. 7).

This hypothesis implies that the moieties of a bupivacine molecule interacting with D1-S6 and D3-S6 are interchangeable whereas the moiety interacting with D4-S6 is not, and, more importantly, that N434 in D1-S6 and L1280 in D3-S6 face each other while interacting with LAs in the inactivated state, but not necessarily in the resting state. The increase in LA affinity during inactivation might be entirely caused by the alignment of these two residues.

In conclusion, our data provide more evidence that in addition to residues in segment D4-S6, residues N434 in D1-S6 and L1280 in D3-S6 both contribute to the high-affinity binding site for local anesthetics in inactivated Na$^+$ channels.

References

Catterall WA (2000) From ionic currents to molecular mechanisms: the structure and function of voltage-gated sodium channels. *Neuron* **26:**13–25.
Cha A, Ruben PC, George AL Jr, Fujimoto E, and Bezanilla F (1999) Voltage sensors in domains III and IV, but not I and II, are immobilized by Na+ channel fast inactivation. *Neuron* **22:**73–87.
Eaholtz G, Scheuer T, and Catterall WA (1994) Restoration of inactivation and block of open sodium channels by an inactivation gate peptide. *Neuron* **12:**1041–1048.
Hille B (1977) Local anesthetics: hydrophilic and hydrophobic pathways for the drug-receptor reaction. *J Gen Physiol* **69:**497–515.
Hondeghem LM and Katzung BG (1977) Time- and voltage-dependent interactions of antiarrhythmic drugs with cardiac sodium channels. *Biochim Biophys Acta* **472:**373–398.
Hopp TP and Woods KR (1981) Prediction of protein antigenic determinants from amino acid sequences. *Proc Natl Acad Sci USA* **78:**3824–3828.
Jiang Y, Lee A, Chen J, Cadene M, Chait BT, and MacKinnon R (2002) The open pore conformation of potassium channels. *Nature (Lond)* **417:**523–526.
Kontis KJ, Rounaghi A, and Goldin AL (1997) Sodium channel activation gating is affected by substitutions of voltage sensor positive charges in all four domains. *J Gen Physiol* **110:**391–401.
Li HL, Galue A, Meadows L, and Ragsdale DS (1999) A molecular basis for the different local anesthetic affinities of resting versus open and inactivated states of the sodium channel. *Mol Pharmacol* **55:**134–141.
McPhee JC, Ragsdale DS, Scheuer T, and Catterall WA (1994) A mutation in segment IVS6 disrupts fast inactivation of sodium channels. *Proc Natl Acad Sci USA* **91:**12346–12350.
McPhee JC, Ragsdale DS, Scheuer T, and Catterall WA (1995) A critical role for transmembrane segment IVS6 of the sodium channel alpha subunit in fast inactivation. *J Biol Chem* **270:**12025–12034.
McPhee JC, Ragsdale DS, Scheuer T, and Catterall WA (1998) A critical role for the S4–S5 intracellular loop in domain IV of the sodium channel alpha-subunit in fast inactivation. *J Biol Chem* **273:**1121–1129.
Nau C, Wang SY, Strichartz GR, and Wang GK (1999) Point mutations at N434 in D1–S6 of mu1 Na$^+$ channels modulate binding affinity and stereoselectivity of local anesthetic enantiomers. *Mol Pharmacol* **56:**404–413.
Perozo E, Cortes DM, and Cuello LG (1999) Structural rearrangements underlying K+-channel activation gating. *Science (Wash DC)* **285:**73–78.
Ragsdale DS, McPhee JC, Scheuer T, and Catterall WA (1994) Molecular determinants of state-dependent block of Na$^+$ channels by local anesthetics. *Science (Wash DC)* **265:**1724–1728.
Sheets MF, Kyle JW, Kallen RG, and Hanck DA (1999) The Na channel voltage sensor associated with inactivation is localized to the external charged residues of domain IV, S4. *Biophys J* **77:**747–757.
Smith MR and Goldin AL (1997) Interaction between the sodium channel inactivation linker and domain III S4–S5. *Biophys J* **73:**1885–1895.
Stuhmer W, Conti F, Suzuki H, Wang XD, Noda M, Yahagi N, Kubo H, and Numa

L1280E, L1280Q, and L1280N was 7, 5, 4, and 2, respectively. The amount of stereoselectivity $[S(-)/R(+)]$ for N434R, N434E, and N434Q was 3, 2.5, and 1.1, respectively. This suggests that in inactivated channels, the chiral part of a bupivacine molecule may be closer to L1280 in D3-S6 than to N434 in D1-S6.

The minimal structural requirement for a drug-receptor interaction to express stereoselectivity is involvement of three groups linked to the chiral center of a drug in interaction with the binding site. Consistent with these requirements, a bupivacaine molecule interacts with residues in D1-S6, D3-S6, and D4-S6 of the Na$^+$ channel. The most critical component of the high-affinity local anesthetic binding site might be segment D4-S6, containing the aromatic residue phenylalanine. Mutations of this phenylalanine caused the most dramatic reduction in the block of inactivated channels (Ragsdale et al., 1994; Wright et al., 1998). Furthermore, segment D4-S6 might be the least mobile of all S6 segments because of the lack of a critical glycine residue

S (1989) Structural parts involved in activation and inactivation of the sodium channel. *Nature (Lond)* **339:**597–603.

Vassilev PM, Scheuer T, and Catterall WA (1988) Identification of an intracellular peptide segment involved in sodium channel inactivation. *Science (Wash DC)* **241:**1658–1661.

Wang GK, Quan C, and Wang SY (1998) Local anesthetic block of batrachotoxin-resistant muscle Na$^+$ channels. *Mol Pharmacol* **54:**389–396.

Wang SY, Barile M, and Wang GK (2001) Disparate role of Na$^+$ channel D2–S6 residues in batrachotoxin and local anesthetic action. *Mol Pharmacol* **59:**1100–1107.

Wang SY, Nau C, and Wang GK (2000) Residues in Na$^+$ channel D3–S6 segment modulate both batrachotoxin and local anesthetic affinities. *Biophys J* **79:**1379–1387.

West JW, Patton DE, Scheuer T, Wang Y, Goldin AL, and Catterall WA (1992) A cluster of hydrophobic amino acid residues required for fast Na$^+$-channel inactivation. *Proc Natl Acad Sci USA* **89:**10910–10914.

Wright SN, Wang SY, and Wang GK (1998) Lysine point mutations in Na$^+$ channel D4–S6 reduce inactivated channel block by local anesthetics. *Mol Pharmacol* **54:**733–739.

Wright SN, Wang SY, Xiao YF, and Wang GK (1999) State-dependent cocaine block

of sodium channel isoforms, chimeras and channels coexpressed with the beta1 subunit. *Biophys J* **76:**233–245.

Yang N, George AL Jr, and Horn R (1996) Molecular basis of charge movement in voltage-gated sodium channels. *Neuron* **16:**113–122.

Yang N and Horn R (1995) Evidence for voltage-dependent S4 movement in sodium channels. *Neuron* **15:**213–218.

Yarov-Yarovoy V, Brown J, Sharp EM, Clare JJ, Scheuer T, and Catterall WA (2001) Molecular determinants of voltage-dependent gating and binding of pore- blocking drugs in transmembrane segment IIIS6 of the Na$^+$ channel alpha subunit. *J Biol Chem* **276:**20–27.

Yarov-Yarovoy V, McPhee JC, Idsvoog D, Pate C, Scheuer T, and Catterall WA (2002) Role of amino acid residues in transmembrane segments IS6 and IIS6 of the Na$^+$ channel alpha subunit in voltage-dependent gating and drug block. *J Biol Chem* **277:**35393–35401.

Address correspondence to: Dr. Carla Nau, Department of Anesthesiology, Friedrich-Alexander-University Erlangen-Nuremberg, Krankenhausstr. 12, 91054 Erlangen, Germany. E-mail: Carla.Nau@kfa.imed.uni-erlangen.des